Proceedings of the 2024 8th CAA International Conference on Vehicular Control and Intelligence (CVCI), Chongqing, China, October 25-27, 2024

Adaptive finite-time prescribed performance accurate tracking control of vehicular platoons with multilevel threshold

1st Zhenyu Gao
School of Control Engineering
Northeastern University
Shenyang, China
18840839109@163.com

2nd Wei Liu
School of Control Engineering
Northeastern University
Shenyang, China
liu_w1999@163.com

3rd Zhongyang Wei
School of Control Engineering
Northeastern University
Shenyang, China
15953603659@163.com

4th Ge Guo
State Key Laboratory of SAPI
Northeastern University
Shenyang, China
geguo@yeah.net

2024 8th CAA International Conference on Vehicular Control and Intelligence (CVCI) | 979-8-3315-0489-2/24/$31.00 ©2024 IEEE | DOI: 10.1109/CVCI63518.2024.10830255

***Abstract*—The issue of prescribed performance platoon control of connected vehicles with dynamic performance threshold is investigated in this paper. A continuous gain function is introduced, combining with finite-time performance function, a novel prescribed performance control (PPC) scheme is developed to make the tracking error tend to the prescribed region with different threshold within the user-defined time. Then, a new finite-time reaching law is proposed, based on which, an improved finite-time sliding mode platoon control algorithm is proposed. The suggested control strategy not only ensures finite-time individual vehicle stability and finite-time string stability, but also realizes the asymptotic convergence of the spacing tracking error. Eventually, the feasibility of the proposed scheme are validated by numerical simulations.**

***Index Terms*—Vehicular platoon, finite-time stability, sliding mode control, asymptotic convergence, prescribed performance control, multilevel threshold.**

I. Introduction

PLATOON control of connected vehicles has attracted many attentions of scholars in the past few years [1], [2], and many advanced control algorithms have been presented, for example SMC [3], backstepping control [4], model predictive control [5], and many others.

It should be noted that only satisfactory steady-state system performance can be obtained by the above control methods, while the transient performance is also crucial for the platooning of vehicles [6]. For this purpose, the prescribed performance control (PPC) were adopted, based on which the transient and steady-state performance of the system all be ensured better [6]–[11]. However, these works only effective for the platoon system with fixed threshold. It is well known that to avoid collisions between adjacent vehicles, the allowable spacing error threshold must be different at high or low speeds. Therefore, PPC methods using a fixed threshold may result in conservative parameter selection, which limits the error to a wide range and hinders the control effectiveness.

The convergence time is another core index to evaluate the vehicle platoon control strategy [12], [13]. Up to today, many advance control methods have been developed, including finite-time controller [10], [11], fixed-time controller [8], [9], and improved versions of the above controllers [13]. Although the desired platoon objective can be achieved within a predefined time by these results, only the boundedness of the tracking errors was ensured. That is, the errors can approach a residual set but cannot reach the origin. As the demand for control accuracy continues to grow, nothing is more attractive than zero tracking error, which also means that the previous method is no longer applicable. Thus, finite-time asymptotic tracking control of vehicular platoons has been recognized as a meaningful yet unresolved problem, providing further motivation for this study.

In order to response to the shortcomings of the existing results, we will investigate finite-time prescribed performance control of vehicular platoons with dynamic threshold by a novel finite-time asymptotic SMC approach. In comparison with the existing results, the primary contributions are summarized as follows:

1) A novel PPC scheme is proposed that synthesizes a continuous gain function together with a newly finite-time performance function, which can guarantee that tracking errors converge to a predefined region with different threshold within user-designed time.
2) A new finite-time sliding mode tracking platoon control method is designed to compel the tracking error converge to a small region nearby zero within settling time, and eventually approach to origin asymptotically.

II. Problem Formation

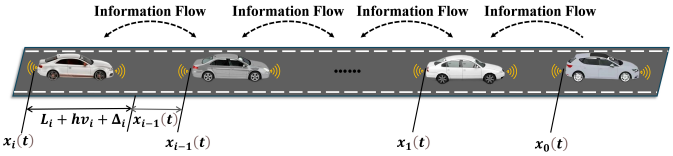

Fig. 1. The heterogeneous vehicular platoon based on BD communication topology.

In this paper, as depicted in Fig. 1, a vehicular platoon with one leader and N followers is considered, utilizing a bidirectional (BD) communication topology.

A. Vehicle Model

As in [14], the following third-order nonlinear model is adopted for vehicle i ($1 \leq i \leq N$):

$$\begin{aligned} \dot{x_i}(t) &= v_i(t) \\ \dot{v_i}(t) &= a_i(t) \\ \dot{a_i}(t) &= f_i(v_i, a_i, t) + u_i(t) + \omega_i(t) \end{aligned} \tag{1}$$

where $x_i(t), v_i(t)$, and $a_i(t)$ represent the position, velocity, and acceleration, respectively. $u_i(t)$ corresponds to the braking/throttling input, $\omega_i(t)$ denotes the external disturbance, and $f_i(v_i, a_i, t)$ denotes the unknown nonlinear dynamics, which is expressed as:

$$\begin{aligned} f_i(v_i, a_i, t) = &- \frac{1}{m_i \tau_i}\Big[\rho_a A_i C_{ai}\left(\frac{1}{2}v_i^2 + \tau_i v_i a_i\right) \\ &+ m_i g b_i \cos\delta_i + m_i g \sin\delta_i\Big] - \frac{1}{\tau_i}a_i \end{aligned}$$

wherein the definition of parameters are given in Table I.

TABLE I
THE DEFINITION OF EACH PARAMETER FOR A VEHICLE

Parmeter	Description	Parmeter	Description
m_i	the mass of vehicle	τ_i	the engine time constant
ρ_a	the air density	δ_i	the road slope angle
C_{ai}	the drag coefficient	A_i	the frontal cross-area
g	the acceleration of gravity	b_i	the road resistance coefficient

Inspired by [15], rewrite (1) as

$$\dot{a}_i(t) = f_{i0}(v_i, a_i, t) + u_i(t) + D_i(t) \tag{2}$$

where $f_{i0}(v_i, a_i, t)$ and $\Delta f_i(v_i, a_i, t)$ represent the known term and the uncertain term, respectively, and $f_i(v_i, a_i, t) = f_{i0}(v_i, a_i, t) + \Delta f_i(v_i, a_i, t)$. $D_i(t) = \Delta f_i(v_i, a_i, t) + \omega_i(t)$ denotes the lumped disturbance acting on vehicle i.

Assumption 1: The disturbance D_i is limited, where $|D_i(t)| \leq \bar{D}_i$ with $\bar{D}_i$ being a positive constant of unknown value.

To generate the reference trajectory for the platoon, the dynamics of leader is described by:

$$\dot{x}_0(t) = v_0(t),\ \dot{v}_0(t) = a_0(t). \tag{3}$$

The inter-vehicle spacing error, denoted as $e_i(t)$, is given by the following definition:

$$e_i(t) = x_{i-1}(t) - x_i(t) - L_i - \Delta_i - h_i v_i(t) \tag{4}$$

where L_i stands for the length of the vehicle, Δ_i represents the minimum safe distance among adjacent vehicles, and h_i indicates the time headway.

B. Control Objectives

In this paper, we aim to formulate a novel control strategy based on the SMC technique for the vehicular platoon described by (1) and (3), ensuring that

1) *Finite-time Compound individual vehicle stability:* The inter-vehicle spacing error e_i converges to a small region ϵ_i within finite time T_i, and eventually approaches to zero, that is
$$\begin{cases} \lim\limits_{t\to T_i} |e_i(t)| \leq \epsilon_i \\ \lim\limits_{t\to\infty} |e_i(t)| = 0 \end{cases} \tag{5}$$
where ϵ_i and T_i are positive constants.
2) *Finite-time String Stability:* After a given time T_{iS}, the spacing error e_i satisfies
$$0 < \left|\frac{e_{i+1}(t)}{e_i(t)}\right| \leq 1, \forall\, t \geq T_{iS}. \tag{6}$$
3) *Finite-time prescribed performance:* The tracking error tends to the given region $\left(-\underline{\xi}_i\rho_i(\tilde{T}_i), \bar{\xi}_i\rho_i(\tilde{T}_i)\right)$ within finite-time $\tilde{T}_i > 0$, that is
$$-\underline{\xi}_i\rho_i(t) < e_i(t) < \bar{\xi}_i\rho_i(t), \forall t \geq \tilde{T}_i \tag{7}$$
where $\underline{\xi}_i, \bar{\xi}_i$ are positive constants, and $\rho_i(t)$ is performance function.

III. Finite-Time Prescribed Performance Control with Multilevel Threshold

A. Finite-Time Performance Function Design

To guarantee the spacing error $e_i(t)$ converges to a performance region with different boundary, inspired by [16], the following finite-time performance function (FnTPF) is designed:

$$\rho_i(t) = \rho_{i1}(t)\Phi_i(t) \tag{8}$$

with

$$\rho_{i1}(t) = \begin{cases} \lambda_i\left(1 - \frac{\ln(t+1)}{\ln(\bar{T}_{i,1}+1)}\right) + \bar{\rho}_{i1}, & 0 \leq t < \bar{T}_{i,1} \\ \bar{\rho}_{i1}, & t \geq \bar{T}_{i,1} \end{cases} \tag{9}$$

and

$$\Phi_i(t) = \prod_{j=1}^{M} \phi_{i,j}(t) \tag{10}$$

$$\phi_{i,j}(t) = \begin{cases} 1, & t \in [\bar{T}_{i,j}, \underline{T}_{i,j}) \\ 1 - \frac{d_{i,j}}{2}\left(1 + \sin\left(\frac{\pi\left(2t - 2\underline{T}_{i,j} - a_{i,j}\right)}{a_{i,j+1}}\right)\right) & t \in [\underline{T}_{i,j}, \bar{T}_{i,j+1}) \\ 1 - d_{i,j}, & t \in [\bar{T}_{i,j+1}, \underline{T}_{i,j+1}) \end{cases} \tag{11}$$

where $\lambda_i \geq 1$, $\bar{\rho}_{i1}$, $\tilde{T}_i$, M, $a_{i,j}$, $\bar{T}_{i,j}$ and $\underline{T}_{i,j}$ are positive constants. Here, $\bar{\rho}_{i1}$ denotes the threshold at the initial time, M denotes the numbers of threshold, $\prod_1^j (1 - d_{i,j})\,\bar{\rho}_{i1}$ is the threshold j, $\bar{T}_{i,j}$ and $\underline{T}_{i,j}$ denote the start time and the end time of the threshold j for vehicle i, $d_{i,j}$ indicates the adjustment ratio of the threshold from threshold $j-1$ to threshold j, $a_{i,j}$ represents duration of threshold change from threshold $j-1$ to threshold j, and satisfies $\bar{T}_{i,j} = \underline{T}_{i,j-1} + a_{i,j}$.

Remark 1: Compared with the FnTPF with fixed threshold in [6]–[11], the gain function Φ_i is introduced to the FnTPF (8). By adjusting the parameter $d_{i,j}$, the desired threshold can be obtained easily. Meanwhile, the duration of the time-varying process can be regulated only by the parameter $a_{i,j}$.

B. Error Transformation

To meet the control target, we introduce the following error transformation, which converts the constrained error into an unconstrained version:

$$\mathcal{E}_i(t) = \Gamma_i^{-1}\left(\frac{e_i(t)}{\rho_i(t)}\right) \tag{12}$$

with

$$\Gamma_i\left(\mathcal{E}_i\right) = \frac{\underline{\xi_i}\bar{\xi}_i\left(e^{\mathcal{E}_i} - e^{-\mathcal{E}_i}\right)}{\underline{\xi_i}e^{\mathcal{E}_i} + \bar{\xi}_i e^{-\mathcal{E}_i}} \tag{13}$$

where $\mathcal{E}_i(t)$ denotes the transformed error, and $\Gamma_i^{-1}(\bullet)$ is the inverse function of $\Gamma_i(\bullet)$.

Then, one has:

$$\mathcal{E}_i(t) = \frac{1}{2}\ln\frac{\bar{\xi}_i\left(\underline{\xi_i}\rho_i(t) + e_i(t)\right)}{\underline{\xi_i}\left(\bar{\xi}_i\rho_i(t) - e_i(t)\right)}. \tag{14}$$

IV. Controller Design and Stability Analysis

A. Controller Design

To maintain the string stability of the vehicular platoon, we introduce the coupled variable E_i:

$$E_i = \begin{cases} q_i\mathcal{E}_i - \mathcal{E}_{i+1}, & i = 1, \ldots, N-1 \\ q_i\mathcal{E}_i, & i = N. \end{cases} \tag{15}$$

where $q_i > 0$. Note that the convergence of $\mathcal{E}_i$ and E_i are same, that is the variables $\mathcal{E}_i$ and E_i converge to origin simultaneously.

1) Enhanced Sliding Mode Surface Design: To ensure the error $\mathcal{E}_i$ converges at a faster rate, we utilize the following sliding mode surface:

$$S_i = \dot{E}_i + \alpha_{i1}\psi_i\left(E_i\right) + \alpha_{i2}E_i \tag{16}$$

with

$$\psi_i\left(E_i\right) = \begin{cases} \mathrm{sig}^{\kappa_i}\left(E_i\right), & |E_i| \geq \iota_i \\ \beta_{i1}E_i + \beta_{i2}E_i^2\mathrm{sign}\left(E_i\right), & |E_i| < \iota_i \end{cases} \tag{17}$$

where $\alpha_{i1} > 0$, $\alpha_{i2} > \frac{1}{2}$, $\iota_i > 0$, $0 < \kappa_i < 1$, $\beta_{i1} = (2-\kappa_i)\iota_i^{\kappa_i - 1}$, $\beta_{i2} = (\kappa_i - 1)\iota_i^{\kappa_i - 2}$, $\mathrm{sig}^{\kappa_i}(E_i) = |E_i|^{\kappa_i}\mathrm{sign}(E_i)$

2) Finite-time sliding mode controller design: To achieve the control objective, the following reaching law is introduced:

$$\dot{S}_i = -\sigma_i\left(K_{i1}S_i + K_{i2}\left|S_i\right|^{p_i}\mathrm{sign}\left(S_i\right)\right) \tag{18}$$

where $\sigma_i = e^{-\varpi_i t}$, K_{i1}, K_{i2} and ϖ_i are positive constants with $0 < p_i < 1$.

Further, on the basis of (18), the controller u_i and the adaptation law $\dot{\hat{D}}_i$ are designed as follows:

$$\begin{aligned} u_i = &\frac{\sigma_i}{q_i h_i R_i}\left[K_{i1}S_i + K_{i2}\left|S_i\right|^{p_i}\mathrm{sign}\left(S_i\right) + Z_i\right] + \\ &\frac{q_i h_i R_i \hat{\bar{D}}_i}{\sqrt{S_i^2 + \sigma_i^2}} + \frac{K_{i1}\left|S_i\right|^{p_i}\mathrm{sign}\left(S_i\right)}{q_i h_i R_i} \end{aligned} \tag{19}$$

$$\dot{\hat{\bar{D}}}_i = \frac{q_i h_i R_i S_i}{\sqrt{S_i^2 + \sigma_i^2}} - \sigma_i\left(K_{i3}\hat{\bar{D}}_i + K_{i4}\hat{\bar{D}}_i^{p_i}\right) \tag{20}$$

where K_{i3} and K_{i4} are positive constants, $R_i = \frac{1}{2}\left(\frac{1}{e_i(t)+\underline{\xi_i}\rho_i(t)} + \frac{1}{\bar{\xi}_i\rho_i(t) - e_i(t)}\right) > 0$, and Z_i is given by

$$Z_i = \begin{cases} q_i\left[R_i\left(-\frac{(\dot{e}_i\dot{\rho}_i + e_i\ddot{\rho}_i)\rho_i - e_i\dot{\rho}_i^2}{\rho_i^2}\right)\right. \\ +R_i\left(a_{i-1} - a_i\right) - h_i R_i f_{i0}\left(v_i, a_i\right) \\ \left.+\alpha_{i2}\dot{R}_i\left(\dot{e}_i - \frac{e_i\dot{\rho}_i}{\rho_i}\right) + \alpha_{i1}\dot{\psi}_i\right] \\ -\ddot{\mathcal{E}}_{i+1} - \alpha_{i2}\dot{\mathcal{E}}_{i+1}, \quad i = 1, 2, \cdots, N-1, \\ q_i\left[R_i\left(-\frac{(\dot{e}_i\dot{\rho}_i + e_i\ddot{\rho}_i)\rho_i - e_i\dot{\rho}_i^2}{\rho_i^2}\right)\right. \\ +R_i\left(a_{i-1} - a_i\right) - h_i R_i f_{i0}\left(v_i, a_i\right) \\ \left.+\alpha_{i2}R_i\left(\dot{e}_i - \frac{e_i\dot{\rho}_i}{\rho_i}\right) + \alpha_{i1}\dot{\psi}_i\right], i = N. \end{cases} \tag{21}$$

B. Stability Analysis

Theorem 1: Consider the vehicular platoon control system (1)-(3) under Assumption 1. With the help of the given control scheme, including the performance functions (8)-(**??**), error transformation (12)-(14), the coupled variable (15), improved sliding mode surface (16), (17), finite-time asymptotic convergence controller (19) and adaptive law (20), we have.

1) All signals of the closed-loop vehicular system can converge to the neighborhood of the origin within a time T_i. Meanwhile, the tracking errors e_i $(1 \leq i \leq N)$ will tend to zero in the end.
2) Finite-time string stability can be guaranteed if the parameter q_i satisfies $0 < q_i < 1$.
3) The performance constraint with multilevel threshold also can be ensured with finite-time.

Proof: The demonstration of *Theorem 1* is carried out through the following three parts.

Part 1: Compound individual vehicle stability: Consider the following Lyapunov function

$$V_{iS} = \frac{1}{2}S_i^2 + \frac{1}{2}\tilde{\bar{D}}_i^2 \tag{22}$$

where $\tilde{\bar{D}}_i = \bar{D}_i - \hat{\bar{D}}_i$ is the estimation error.

Taking the time derivative of V_i yields:

$$\dot{V}_{iS} = S_i\dot{S}_i - \tilde{\bar{D}}\dot{\hat{\bar{D}}}. \tag{23}$$

Combining (1), (2) and (19), the time derivative of $S_i(t)$ is given as follow:

$$\begin{aligned} \dot{S}_i(t) = &-\left[K_{i1}S_i + (1+\sigma_i)K_{i2}\left|S_i\right|^{p_i}\mathrm{sign}\left(S_i\right) + \frac{q_i h_i R_i \hat{\bar{D}}_i}{\sqrt{S_i^2 + \sigma_i^2}}\right] \\ &- q_i h_i R_i D_i. \end{aligned} \tag{24}$$

Then, we have

$$\begin{aligned} S_i\dot{S}_i =& -\sigma_i K_{i1}S_i^2-(1+\sigma_i)K_{i2}|S_i|^{p_i}S_i\text{sign}(S_i) \\ & -\frac{q_ih_iR_i\hat{\bar{D}}_iS_i}{\sqrt{S_i^2+\sigma_i^2}}-q_ih_iR_iD_iS_i. \end{aligned} \tag{25}$$

Based on (20), (23) and (25), one has

$$\begin{aligned} \dot{V}_{iS} =& -\sigma_i K_{i1}S_i^2-(1+\sigma_i)K_{i2}|S_i|^{p_i}S_i\text{sign}(S_i) \\ & -\sigma_i\tilde{\bar{D}}_i\left(K_{i3}\hat{\bar{D}}_i+\sigma_iK_{i4}\hat{\bar{D}}_i^{p_i}\right) \\ & -\frac{q_ih_iR_i\bar{D}_iS_i}{\sqrt{S_i^2+\sigma_i^2}}-q_ih_iR_iD_iS_i. \end{aligned} \tag{26}$$

Based on Assumption 1, the following inequality can be obtained:

$$-q_ih_iR_iS_iD_i \le q_ih_iR_i\bar{D}_i\left|S_i\right|. \tag{27}$$

Using the Lemma 5 in [17], one has:

$$q_ih_iR_i\bar{D}_i\left|S_i\right|-\frac{q_ih_iR_i\bar{D}_iS_i}{\sqrt{S_i^2+\sigma_i^2}} \le q_ih_iR_i\bar{D}_i\sigma_i. \tag{28}$$

Based on the Lemma 3 in [11], $\tilde{\bar{D}}_i\hat{\bar{D}}_i^{p_i}$ satisfies the following inequality:

$$\hat{D}_i^{p_i}\left(\bar{D}_i-\hat{\bar{D}}_i\right) \le -\frac{1}{1+p_i}\tilde{\bar{D}}_i^{1+p_i}+\frac{2}{1+p_i}\bar{D}_i^{1+p_i}. \tag{29}$$

Substituting (27), (28) and (29) into (26), one has:

$$\begin{aligned} \dot{V}_{iS} \le& -\sigma_i\left[K_{i2}2^{\frac{1+p_i}{2}}\left(\frac{S_i^2}{2}\right)^{\frac{1+p_i}{2}}+\frac{K_{i4}}{1+p_i}2^{\frac{1+p_i}{2}}\left(\frac{\tilde{\bar{D}}_i^2}{2}\right)^{\frac{1+p_i}{2}}\right] \\ & -\sigma_i\left(2K_{i1}\frac{S_i^2}{2}+2K_{i3}\frac{\tilde{\bar{D}}_i^2}{2}\right)+2\sigma_iK_{i3}\bar{D}_i^2 \\ & +\frac{2\sigma_iK_{i4}}{1+p_i}\bar{D}_i^{1+p_i}-\sigma_iq_ih_iR_i\bar{D}_i-K_{i2}|S_i|^{p_i+1} \end{aligned} \tag{30}$$

In the light of Lemma 1 in [10], we have

$$\dot{V}_{iS} \le \sigma_i\left(-\nu_iV_{iS}-\eta_iV_{iS}^{\frac{1+p_i}{2}}+\varrho_i\right) \tag{31}$$

where

$$\begin{aligned} \nu_i &= \min\left\{2K_{i1},2K_{i3}\right\} \\ \eta_i &= \min\left\{K_{i2}2^{\frac{1+p_i}{2}},\frac{K_{i4}}{1+p_i}2^{\frac{1+p_i}{2}}\right\} \\ \varrho_i &= 2K_{i3}\bar{D}_i^2+\frac{2K_{i4}}{1+p_i}\bar{D}_i^{1+p_i}-q_ih_iR_i\bar{D}_i. \end{aligned} \tag{32}$$

According to Lemma 1 in [18], it is conclude that V_{iS} is finite-time stable, thus, the signals S_i and $\tilde{\bar{D}}_i$ will converge to the compact set Ω_i within finite time T_{iS}, wherein Ω_i and T_{iS} are expressed as follows:

$$\left\{|S_i|,|\tilde{\bar{D}}_i|\right\} \le \Omega_i := \min\left\{\frac{\varrho_i}{(1-\theta_i)\nu_i},\left(\frac{\varrho_i}{(1-\theta_i)\eta_i}\right)^{\frac{2}{1+p_i}}\right\} \tag{33}$$

and

$$T_{iS} \le T_{\max} := \max\left\{\tilde{T}_1,\tilde{T}_2\right\} \tag{34}$$

with

$$\tilde{T}_1=\frac{1}{\varpi_i}\frac{\nu_i\theta_i(1-p_i)}{2\varpi_i\left(\ln\frac{\nu_i\theta_i\left(\frac{\varrho_i}{(1-\theta_i)\nu_i}\right)^{\frac{1-p_i}{2}}+\eta_i}{\nu_i\theta_iV_{iS}^{\frac{1-p_i}{2}}(0)+\eta_i}\right)+\varpi_i\nu_i\theta_i(1-p_i)} \tag{35}$$

and

$$\tilde{T}_2=\frac{1}{\varpi_i}\frac{\nu_i\theta_i(1-p_i)}{2\varpi_i\left(\ln\frac{\nu_i\theta_i\left(\frac{\varrho_i}{(1-\theta_i)\nu_i}\right)^{\frac{1-p_i}{1+p_i}}+\eta_i\theta_i}{\nu_iV_{iS}^{\frac{1-p_i}{2}}(0)+\eta_i\theta_i}\right)+\varpi_i\nu_i\theta_i(1-p_i)} \tag{36}$$

where $0<\theta_i<1$.

Integrate (31) from 0 to t :

$$\eta_i\int_0^t\left(\frac{S_i^2}{2}\right)^{\frac{1+p_i}{2}}d\tau \le V_{iS}(0)+\varrho_i\frac{1-e^{-\varpi_it}}{\varpi_i} \tag{37}$$

Further, we have

$$\lim_{t\to+\infty}\eta_i\int_0^t\left(\frac{S_i^2}{2}\right)^{\frac{1+p_i}{2}}d\tau \le V_{iS}(0)+\frac{\varrho_i}{\varpi_i}<\infty. \tag{38}$$

By using Lemma 2 in [18], we can infer that $\lim_{t\to\infty}S_i=0$. Based on above analysis, one can obtain

$$\begin{cases}\lim\limits_{t\to T_{iS}}|S_i|=\Omega_i \\ \lim\limits_{t\to\infty}|S_i|=0.\end{cases} \tag{39}$$

Next, the convergence of E_i will be proved by the following two discussions.

Discussion 1: When $S_i=\Delta_i$, sliding mode surface (16) can be rewritten as:

$$\dot{E}_i=-\alpha_{i1}\psi_i\left(E_i\right)-\alpha_{i2}E_i+\Delta_i. \tag{40}$$

Consider the following Lyapunov function

$$V_{iE}=\frac{1}{2}E_i^2 \tag{41}$$

and taking the time derivative of V_{iE}, one has

$$\dot{V}_{iE}=E_i\dot{E}_i. \tag{42}$$

Considering the relationships between $|E_i|$ and ι_i in (17), we will analyse the convergence of E_i separately.

Here, the similar analysis can be referred to [11], thus it is omitted in this paper.

Discussion 2: When $S_i=0$ as shown in (45), sliding mode surface (16) becomes

$$\dot{E}_i=-\alpha_{i1}\psi_i\left(E_i\right)-\alpha_{i2}E_i. \tag{43}$$

In the same way, the analysis of $\mathcal{E}_i$ is same with **Discussion 1**, it is also omitted here.

By applying Lemma 1 in [19], $\mathcal{E}_i$ converges to zero in finite time $T_{i\mathcal{E}}$, satisfies

$$T_{i\mathcal{E}} \le \frac{1}{\alpha_{i2}\left(1-\kappa_i\right)}\ln\frac{2\alpha_{i2}V_{i\mathcal{E}}^{(1-\kappa_i)/2}(0)+2^{(\kappa_i+1)/2}\alpha_{i1}}{2^{(\kappa_i+1)/2}\alpha_{i1}}. \tag{44}$$

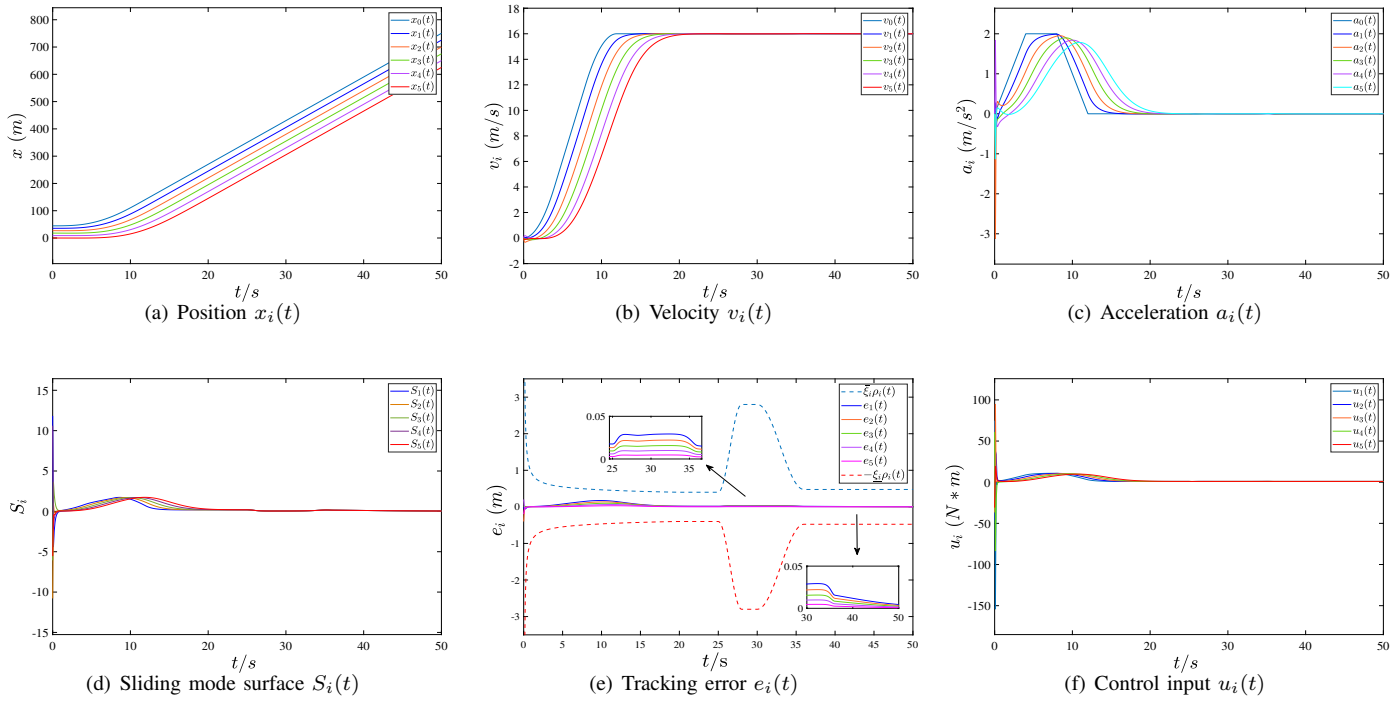

(a) Position $x_i(t)$ (b) Velocity $v_i(t)$ (c) Acceleration $a_i(t)$

(d) Sliding mode surface $S_i(t)$ (e) Tracking error $e_i(t)$ (f) Control input $u_i(t)$

Fig. 2. Simulation results of the proposed method.

Since E_i and $\mathcal{E}_i$ have the same convergence, thus there exists a positive constant Δ_i such that

$$\begin{cases} \lim\limits_{t\to T_{i\mathcal{E}}} |\mathcal{E}_i| = \Delta_i \\ \lim\limits_{t\to\infty} |\mathcal{E}_i| = 0. \end{cases} \tag{45}$$

In addition, due to $\mathcal{E}_i$ and e_i are equivalent, there exists ϵ_i and $T_i > T_{iS} + T_{i\mathcal{E}}$ such that $\lim\limits_{t\to T_i} |e_i(t)| \leq \epsilon_i$ and $\lim\limits_{t\to\infty} |e_i(t)| = 0$, which indicates that the compound individual vehicle stability (5) is guaranteed.

Part 2: Finite-time String stability: Since $E_i = q_i\mathcal{E}_i - \mathcal{E}_{i+1}$, once E_i converges to the origin, we have

$$\frac{\mathcal{E}_{i+1}}{\mathcal{E}_i} = q_i. \tag{46}$$

Since e_i and $\mathcal{E}_i$ are equivalent, combining $q_i \in (0, 1]$, we have $0 < |(e_{i+1}/e_i)| \leq 1$, which illustrates that string stability can be guaranteed [11].

Part 3: Reachability of prescribed performance (7): Since the tracking error $\mathcal{E}_i(t)$ is finite-time convergent and bounded, thus there must exists a maximum value. Here, defining $\bar{\mathcal{E}}_i$ as the upper bound of $\mathcal{E}_i$.

From (14), it is deduced that:

$$\frac{\bar{\xi}_i\left(\underline{\xi}_i\rho_i(t) + e_i(t)\right)}{\underline{\xi}_i\left(\bar{\xi}_i\rho_i(t) - e_i(t)\right)} = e^{2\mathcal{E}_i}. \tag{47}$$

Then

$$\frac{e_i(t) + \underline{\xi}_i\rho_i(t)}{\bar{\xi}_i\rho_i(t) + \underline{\xi}_i\rho_i(t)} = \frac{\underline{\xi}_i e^{2\mathcal{E}_i}}{\bar{\xi}_i + \underline{\xi}_i e^{2\mathcal{E}_i}}. \tag{48}$$

Due to $\bar{\mathcal{E}}_i \geq \mathcal{E}_i$, we have

$$0 < \frac{\underline{\xi}_i e^{-2\bar{\mathcal{E}}_i}}{\bar{\xi}_i + \underline{\xi}_i e^{-2\bar{\mathcal{E}}_i}} < \frac{\underline{\xi}_i e^{2\mathcal{E}_i}}{\bar{\xi}_i + \underline{\xi}_i e^{2\mathcal{E}_i}} < \frac{\underline{\xi}_i e^{2\bar{\mathcal{E}}_i}}{\bar{\xi}_i + \underline{\xi}_i e^{2\bar{\mathcal{E}}_i}} < 1. \tag{49}$$

Further, it follows that $0 < \frac{e_i(t)+\underline{\xi}_i\rho_i(t)}{\bar{\xi}_i\rho_i(t)+\underline{\xi}_i\rho_i(t)} < 1$, so $-\underline{\xi}_i\rho_i(t) < e_i(t) < \bar{\xi}_i\rho_i(t)$.

According to the characteristic of (8), it is obvious that the tracking error $e_i(t)$ converges to the region $\left(-\underline{\xi}_i\rho_i(\tilde{T}_i), \bar{\xi}_i\rho_i(\tilde{T}_i)\right)$ within finite-time $\tilde{T}_i > 0$. Thus, the predefined tracking performance outlined in (7) is ensured.

The complete proof of Theorem 1 is achieved through the three sections discussed above. ■

V. Simulation Studies

In this section, we perform numerical simulations on the vehicular platoon system, consisting of $N = 5$ following vehicles and one leader, to illustrate the effectiveness of the proposed method. The vehicle parameters are chosen as follows: $m_i = 1600kg$, $A_i = 2.2m^2$, $\rho_a = 0.2$, $\tau_i = 0.2$, $C_{ai} = 0.35$, $g = 9.8m/s^2$, $\delta_i = 0$, $b_i = 0.02$, $\omega_i = 0.1\tanh(t)$, $f_{i0}(v_i, a_i) = 2\Delta f_i(v_i, a_i)$, and the platoon parameters are chosen as: $\Delta_i = 7m$, $h_i = 1s$ and $L_i = 2m$, The initial states (i.e., positions and velocities) are selected as: $x_i(0) = [45, 36.2, 27.5, 17.8, 9.2, 0]m$, and $v_i(0) = 0m/s$ with $i = 0, 1, \cdots, N$.

The acceleration of leader is designed as:

$$a_0(t) = \begin{cases} 0.5t\ m/s^2, & 0s \le t < 4s \\ 2\ m/s^2, & 4s \le t < 8s \\ -0.5t + 6\ m/s^2, & 8s \le t \le 12s \\ 0\ m/s^2, & t \ge 12s \end{cases} \tag{50}$$

Here, the control parameters of each vehicle are designed as: $q_i = 0.9$, $\kappa_i = 0.8$, $\alpha_{i1} = 12$, $\alpha_{i2} = 8$, $\iota_i = 0.1$, $\underline{\xi}_i = \bar{\xi}_i = 0.4$, $K_{i1} = 3$, $K_{i2} = 80$, $K_{i3} = 1$, $K_{i4} = 1$, $\varpi_i = 0.03$, $p_i = 0.999$.

The dynamic threshold FnTPF parameters are designed as: $\bar{T}_{i,1} = 20$, $\lambda_i = 1$, $\bar{\rho}_{i1} = 1$, $a_{i,1} = 3$, $a_{i,2} = 6$, $\underline{T}_{i,1} = 25$, $\underline{T}_{i,2} = 30$ $d_{i,1} = -6$, $d_{i,2} = 0.6$.

The simulation results are depicted in Fig. 2. The trajectory of each vehicle is presented in Fig. 2(a), which illustrates that the desired platoon configuration can be achieved in finite time. Figs. 2(b) and 2(c) give the velocity and acceleration information of each vehicle, respectively, from which we can see that these two states of each vehicle tend to coincide in a finite time. Figs. 2(d) and 2(e) show the sliding mode surface S_i and tracking error e_i, and these two variables converge to small region nearby zero within finite time. From Fig. 2(g), it is concluded that the tracking errors are always within the predefined region, and no boundary violation occurs. Furthermore, of significant importance is the clear influence of the dynamic threshold predefined performance function on the tracking error. Importantly, it can be clearly seen that the tracking error becomes bigger or smaller as the threshold is adjusted, which indicates that our given PPC algorithm is efficient. In addition, the platoon string stability is also guaranteed, i.e., $|e_{i+1}(t)| < |e_i(t)|$ with $i = 1, 2, 3, 4$. The control input is depicted in Fig. 2(f), which remains constant once the platoon achieved.

VI. Conclusions

The platoon tracking control problem of connected vehicles subject to multilevel prescribed performance constraints is studied. By combining conventional finite-time performance function and novel continuous gain function, a new improved finite-time performance function is designed to compel the tracking errors converge to a predefined region with dynamic performance threshold within finite time. Subsequently, a new finite-time sliding mode control scheme is proposed, under which the tracking error converges to a small region close to zero within finite time and eventually reaches zero. Meanwhile, other two objectives that the string stability and reachability of prescribed performance are also guaranteed.

VII. Acknowledgment

This work was supported by the National Natural Science Foundation of China (62303101) and the Natural Science Foundation of Hebei Province (F2023501001).

References

[1] S. Chu and A. Majumdar, "Opportunities and challenges for a sustainable energy future," *nature*, vol. 488, no. 7411, pp. 294–303, Aug. 2012.

[2] A. Rasouli and J. K. Tsotsos, "Autonomous vehicles that interact with pedestrians: A survey of theory and practice," *IEEE Transactions on Intelligent Transportation Systems*, vol. 21, no. 3, pp. 900–918, Mar. 2020.

[3] Z. Liu and H. Pan, "Barrier function-based adaptive sliding mode control for application to vehicle suspensions," *IEEE Transactions on Transportation Electrification*, vol. 7, no. 3, pp. 2023–2033, 2021.

[4] L. Zhang, H. Ding, J. Shi, Y. Huang, H. Chen, K. Guo, and Q. Li, "An adaptive backstepping sliding mode controller to improve vehicle maneuverability and stability via torque vectoring control," *IEEE Transactions on Vehicular Technology*, vol. 69, no. 3, pp. 2598–2612, Mar. 2020.

[5] M. Wang, C. Zhao, J. Xia, and J. Sun, "Periodic event-triggered robust distributed model predictive control for multiagent systems with input and communication delays," *IEEE Transactions on Industrial Informatics*, vol. 19, no. 11, pp. 11 216–11 228, Nov. 2023.

[6] C.-L. Zhang and G. Guo, "Prescribed performance sliding mode control of vehicular platoons with input delays," *IEEE Transactions on Intelligent Transportation Systems*, pp. 1–9, 2024.

[7] D. Li and G. Guo, "Prescribed performance concurrent control of connected vehicles with nonlinear third-order dynamics," *IEEE Transactions on Vehicular Technology*, vol. 69, no. 12, pp. 14 793–14 802, Dec. 2020.

[8] Z. Gao, Y. Zhang, and G. Guo, "Adaptive fixed-time sliding mode control of vehicular platoons with asymmetric actuator saturation," *IEEE Transactions on Vehicular Technology*, Jul. 2023.

[9] Z. Gao, Y. Zhang, and G. Guo, "Fixed-time prescribed performance adaptive fixed-time sliding mode control for vehicular platoons with actuator saturation," *IEEE Transactions on Intelligent Transportation Systems*, vol. 23, no. 12, pp. 24 176–24 189, Dec. 2022.

[10] Z. Gao, Y. Zhang, and G. Guo, "Finite-time fault-tolerant prescribed performance control of connected vehicles with actuator saturation," *IEEE Transactions on Vehicular Technology*, vol. 72, no. 2, pp. 1438–1448, Feb. 2023.

[11] Z. Sun, Z. Gao, G. Guo, and S. Wen, "Finite-time control of vehicular platoons with global prescribed performance and actuator nonlinearities," *IEEE Transactions on Intelligent Vehicles*, vol. 9, no. 1, pp. 1768–1779, Jan. 2024.

[12] J. Han, J. Zhang, C. He, C. Lv, X. Hou, and Y. Ji, "Distributed finite-time safety consensus control of vehicle platoon with senor and actuator failures," *IEEE Transactions on Vehicular Technology*, vol. 72, no. 1, pp. 162–175, Jan. 2023.

[13] J. Wang, X. Luo, W.-C. Wong, and X. Guan, "Specified-time vehicular platoon control with flexible safe distance constraint," *IEEE Transactions on Vehicular Technology*, vol. 68, no. 11, pp. 10 489–10 503, Nov. 2019.

[14] G. Guo, P. Li, and L.-Y. Hao, "A new quadratic spacing policy and adaptive fault-tolerant platooning with actuator saturation," *IEEE Transactions on Intelligent Transportation Systems*, vol. 23, no. 2, pp. 1200–1212, Feb. 2022.

[15] V. K. Tripathi, A. K. Kamath, L. Behera, N. K. Verma, and S. Nahavandi, "An adaptive fast terminal sliding-mode controller with power rate proportional reaching law for quadrotor position and altitude tracking," *IEEE Transactions on Systems, Man, and Cybernetics: Systems*, vol. 52, no. 6, pp. 3612–3625, Jun. 2022.

[16] X. Liu, H. Zhang, J. Sun, and X. Guo, "Dynamic threshold finite-time prescribed performance control for nonlinear systems with dead-zone output," *IEEE Transactions on Cybernetics*, vol. 54, no. 1, pp. 655–664, Jan. 2024.

[17] Z. Ma and H. Ma, "Adaptive fuzzy backstepping dynamic surface control of strict-feedback fractional-order uncertain nonlinear systems," *IEEE Transactions on Fuzzy Systems*, vol. 28, no. 1, pp. 122–133, Jan. 2020.

[18] Y. Li, Y.-X. Li, and S. Tong, "Event-based finite-time control for nonlinear multiagent systems with asymptotic tracking," *IEEE Transactions on Automatic Control*, vol. 68, no. 6, pp. 3790–3797, Jun. 2023.

[19] A. Polyakov, "Nonlinear feedback design for fixed-time stabilization of linear control systems," *IEEE Transactions on Automatic Control*, vol. 57, no. 8, pp. 2106–2110, Aug. 2012.